Three-Dimensional Linear Viscoelastic Properties of Two Bituminous Mixtures Made with the Same Binder

Daniel Perraton, Hervé Di Benedetto, Cédric Sauzeat, Quang Tuan Nguyen, Simon Pouget

Three-Dimensional Linear Viscoelastic Properties of Two Bituminous Mixtures Made with the Same Binder

Daniel Perraton[1]; Hervé Di Benedetto[2]; Cédric Sauzéat[3]; Quang Tuan Nguyen, Ph.D.[4]; and Simon Pouget[5]

Abstract: Eiffage developed a high-performance bituminous mixture known as GB5. It is based on aggregate optimization method. This paper presents the results of a research project checking whether, in the small strain domain, this type of mixture behaves like the more conventional asphalt mixture GB3 currently used as a base layer in French bituminous pavements. Three-dimensional complex modulus tests are performed on GB5 and GB3, two hot mixtures asphalt (HMA) made with the same bitumen but produced with different aggregate skeletons. Tension-compression sinusoidal testing is applied to the specimens over a wide frequency and temperature range. Both axial and radial strains are monitored, thereby allowing the computation of the complex Young's modulus and complex Poisson's ratios. From the experimental results, the time–temperature superposition principle (TTSP) is verified for both complex Young's modulus and complex Poisson's ratios in two directions. The obtained shift factors and normalized complex modulus curves for the two mixtures indicate that the bitumen phase drives the viscoelastic behaviour of the asphalt mixture, regardless of the granular skeleton. The effect of air-void content on the static, glassy, and characteristic time values of modulus and Poisson's ratios, which is obtained from simulation using a linear viscoelastic model with two springs, two parabolic elements, one dashpot, is analyzed. The anisotropic properties of the two mixtures and the reproducibility between the two laboratories is also checked.

Author keywords: Bituminous mixture; Complex Poisson's ratio; Complex Young's modulus; Modelling; Viscoelastic property; Three-dimensional (3D) behavior.

Introduction

The complex Young's modulus (E^*) and the complex Poisson's ratio (ν^*) are used to define a material's three-dimensional (3D) properties for isotropic linear viscoelastic (LVE) materials. Recently, a detailed review of the literature for the three-dimensional characterization of linear viscoelastic properties of bituminous mixtures was published as state of the art by Task Group 3 (TG3) of RILEM TC 237-SIB (Graziani et al. 2018). Previous studies (Di Benedetto et al. 2001; Airey et al. 2003; Gudmarsson et al. 2014, 2015; Nguyen et al. 2015b, 2017; Perraton et al. 2016; Graziani et al. 2017) showed that classical bituminous mixtures can be considered as LVE if the applied strain amplitude remains small (approximately 10^{-5} m/m). Anisotropy can also be observed for bituminous mixtures but its level remains rather limited (Di Benedetto et al. 2016; Perraton et al. 2016). The present paper investigates the rheological properties of a new type of high-performance asphalt bituminous mixtures known as GB5 and models these properties with a two springs, two parabolic elements, one dashpot (2S2P1D) model developed at the University of Lyon/Ecole Nationale des Travaux Publics de l'Etat (ENTPE) (Lyon, France) (Olard and Di Benedetto 2003; Di Benedetto et al. 2007b).

Behavior of GB5 is compared with that of a classical GB3 French-type hot mix asphalt (HMA) currently used as a base layer, made with the same bitumen. GB5 HMA is obtained by optimizing the mixture of fine and coarse fractions, resulting in an interactive network of coarse particles which provides a strong resistance (Olard and Perraton 2010; Olard et al. 2010; Perraton et al. 2007).

Tension–compression complex modulus tests were performed on both materials in two laboratories: Laboratoire de Tribologie et Dynamique des Systèmes (LTDS) at the University of Lyon/ENTPE (TPE) and Laboratoire sur les Chaussées et Matériaux Bitumineux (LCMB) at the University of Québec/École de Technologie Supérieure (ETS) (Québec, Canada). Results were analyzed. Some properties that may be considered as coming from the binder were shown to be common for the two types of mixtures.

Complex Parameters for Linear Viscoelastic Materials

Definition

The viscoelastic properties of materials can be obtained from sinusoidal loadings applied during the so-called complex modulus test. This paper reports on tests performed on cylindrical samples of axially loaded [Direction 1 (dir)] HMA. To observe linear behavior, the axial strain amplitude was lower than 10^{-4} m/m (Perraton et al. 2016; Di Benedetto et al. 2001; Airey et al. 2003; Nguyen et al. 2015b; Graziani et al. 2014; Godenzoni et al. 2017). In addition to avoid biasing effects such as transient effects

[1]Professor, École de technologie supérieure, Université du Québec, 1100 Notre-Dame St. West, Montréal, QC, Canada H3C 1K3. Email: daniel.perraton@etsmtl.ca

[2]Professor, Ecole Nationale des Travaux Publics de l'Etat-Laboratoire de Tribologie et Dynamique des Systèmes, Université de Lyon, 69518 Vaulx-en-Velin, France. Email: herve.dibenedetto@entpe.fr

[3]Professor, Ecole Nationale des Travaux Publics de l'Etat-Laboratoire de Tribologie et Dynamique des Systèmes, Université de Lyon, 69518 Vaulx-en-Velin, France. Email: cedric.sauzeat@entpe.fr

[4]Lecturer, Dept. of Civil Engineering, Univ. of Transport and Communications, 100000 Hanoi, Vietnam (corresponding author). ORCID: https://orcid.org/0000-0001-5318-0381. Email: quangtuan.nguyen@utc.edu.vn

[5]Research and Innovation Project Manager, Eiffage Infrastructures, 8, rue du Dauphiné, 69960 Corbas, France. Email: simon.pouget@eiffage.com

(Nguyen et al. 2015a; Gayte et al. 2016), self-heating, and thixotropy (Mangiafico et al. 2015; Babadopulos et al. 2017; Riahi et al. 2017) few cycles were applied for each frequency.

For sinusoidal tension/compression loading applied in Direction 1, the axial stress (σ_1), the axial strain (ε_1), and the radial strain values in Directions 2 (dir2) and 3 (dir3) (ε_2 and ε_3, repsectively), can be expressed for linear viscoelastic materials as

$$\varepsilon_1(t) = \varepsilon_{01} \cdot \sin(\omega t + \phi_{\varepsilon 1}) \tag{1}$$

$$\sigma_1(t) = \sigma_{01} \cdot \sin(\omega t + \phi_{\sigma 1}) \tag{2}$$

$$\varepsilon_i(t) = \varepsilon_{0i} \cdot \sin(\omega t + \phi_{\varepsilon i}) \quad (i = 2, 3) \tag{3}$$

where ε_{01}, ε_{02}, ε_{03}, and σ_{01} = axial strain amplitude, radial strain amplitude in Directions 2 and 3, and axial stress amplitude, respectively; $\omega = 2\pi f$ = angular frequency, where fr = frequency; and ϕ = phase angles which can be used to characterize the time shift between the different signals.

Considering exponential notation, the complex Young's modulus in Direction 1 is given by

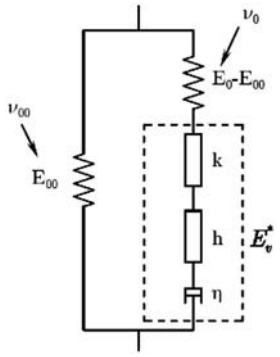

Fig. 1. Analogical representation of 2S2P1D model.

$$E^* = \frac{\sigma_{01}}{\varepsilon_{01}} e^{j(\phi_{\sigma 1} - \phi_{\varepsilon 1})} = |E^*| e^{j\phi_E} \tag{4}$$

where j = complex number defined by $j^2 = -1$.

The complex Poisson's ratios for Directions 2 and 3 are given by

$$\nu_i^* = -\frac{\varepsilon_{0i}}{\varepsilon_{01}} e^{j(\phi_{\varepsilon i} - \phi_{\varepsilon 1})} = \frac{\varepsilon_{0i}}{\varepsilon_{01}} e^{j(\phi_{\varepsilon i} - \phi_{\varepsilon 1} - \pi)} = |\nu_i^*| e^{j\phi_{\nu i}} \quad (i = 2, 3) \tag{5}$$

$$\phi_{\nu i} = \phi_{\varepsilon i} - \phi_{\varepsilon 1} - \pi \tag{6}$$

where ϕ_E = phase angle between axial stress and axial strain; $\phi_{\nu 2}$ and $\phi_{\nu 3}$ = phase angles between the opposite of radial strains in Directions 2 and 3 and the axial strain; and $|E^*|$, $|\nu_2^*|$, and $|\nu_3^*|$ = norms of the complex Young's modulus and of the complex Poisson's ratios in Directions 2 and 3, respectively.

Modeling

Modeling of LVE properties of tested mixtures was done with the 2S2P1D model developed at University of Lyon/ENTPE (Olard and Di Benedetto 2003; Di Benedetto et al. 2007a). The model is based on a simple combination of physical elements (two springs, two parabolic elements, and one dashpot) (Fig. 1). The 2S2P1D model was successfully considered to simulate the linear viscoelastic unidimensional or tridimensional behaviors of bituminous materials (including binders, mastics, and mixtures) (Di Benedetto et al. 2004; Lachance-Tremblay et al. 2016; Lamothe et al. 2017, 2016; Mangiafico et al. 2014; Md. Yusoff et al. 2013; Perraton et al. 2016; Pham et al. 2015a, b; Pouget et al. 2012; Riccardi et al. 2018; Jiménez del Barco Carrión et al. 2017; Aurangzeb et al. 2017).

The complex modulus and the complex Poisson's ratio of the 2S2P1D model at a fixed temperature are respectively

$$E^*_{2S2P1D}(\omega) = E_{00} + \frac{E_0 - E_{00}}{1 + \delta(j\omega\tau_E)^{-k} + (j\omega\tau_E)^{-h} + (j\omega\beta\tau_E)^{-1}} \tag{7}$$

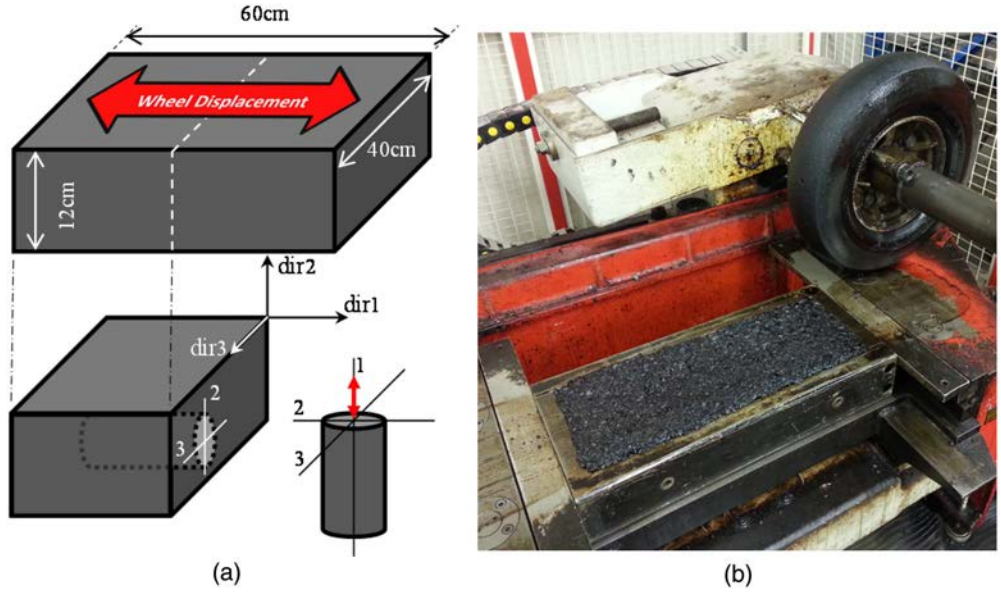

Fig. 2. Diagram of tested specimen production: (a) bituminous mixture specimen obtained from slab; and (b) French LPC compactor used to make bituminous mixture slabs.

$$\nu^*_{2S2P1D}(\omega) = \nu_{00} + \frac{\nu_0 - \nu_{00}}{1 + \delta(j\omega\tau_\nu)^{-k} + (j\omega\tau_\nu)^{-h} + (j\omega\beta\tau_\nu)^{-1}} \tag{8}$$

where k and h = constants, where $0 < k < h < 1$; δ = shape constant; E_{00} = static modulus when $\omega \to 0$; E_0 = glassy modulus when $\omega \to \infty$; ν_{00} = static Poisson's ratio when $\omega \to 0$; ν_0 = glassy Poisson's ratio when $\omega \to \infty$; $\eta = (E_0 - E_{00})\beta\tau_E$ = Newtonian viscosity of the dashpot; β = parameter linked with η; and τ_E and τ_ν = characteristic time values, which are the only parameters depending on temperature

$$\tau_E(T) = a_{TE}(T) \cdot \tau_{0E} \quad \text{and} \quad \tau_\nu(T) = a_T(T) \cdot \tau_{0\nu} \tag{9}$$

where a_{TE} = shift factor at temperature T; and $\tau_E = \tau_{0E}$ and $\tau_\nu = \tau_{0\nu}$ at reference temperature T_{ref}. Ten constants (E_{00}, E_0, δ, k, h, β, ν_{00}, ν_0, τ_{0E}, $\tau_{0\nu}$) are required to completely characterize the 3D LVE properties (with isotropy hypothesis) at a given temperature. When the temperature effect is considered, the number of constants rises to twelve, including the two Williams–Landel–Ferry (WLF) constants (C_1 and C_2) [Eq. (10)].

Experimental Program

Complex Young's modulus and Poisson's ratio measurements were carried out in TPE and LCMB. Bituminous mixture slabs ($120 \times 400 \times 600$ mm^3) were provided by the laboratory of Eiffage (Vélizy-Villacoublay, France).

Tested Material and Sample Preparation

Two bituminous mixtures, GB3 and GB5, were tested. These mixtures are used for base-course construction in France. Bituminous mixtures were produced in the laboratory according to the NF EN 12697-33 and 35 standards (CEN 2007a, b).

Cylindrical asphalt samples were cored from slabs compacted in the laboratory with a French LPC compactor (Fig. 2). The plane surface of each specimen was properly marked to situate the location of Directions 2 and 3 [Fig. 2(b)]. The preferential material Directions 1 (wheel rolling displacement), 2 (vertical), and 3 (perpendicular to Directions 1 and 2) are shown in Fig. 2(a).

A nominal aggregate size of 0–14 mm with high-quality, fully-crushed aggregates and a 35/50 Pen grade pure bitumen was used. The same bitumen and aggregate sources were used for both mixtures. The bitumen content was 4.5% by weight of the mixture for both mixtures (GB3 and GB5). Fig. 3 presents the aggregate grading curve of GB3 and GB5 bituminous mixtures. The maximum specific gravity of the mixtures (G_{mm}) was 2.670 and 2.654 for the GB3 and GB5 mixtures, respectively. The geometrical characteristics of the tested specimens are listed in Table 1.

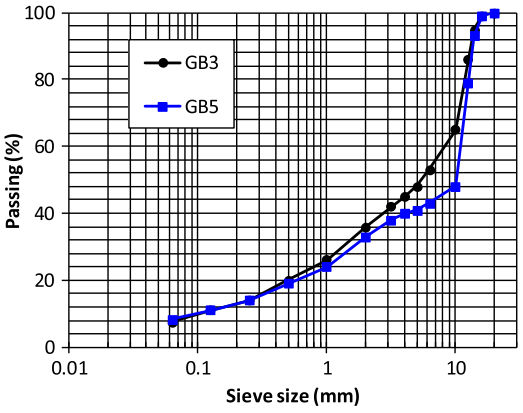

Fig. 3. Grading curves of tested GB3 and GB5 bituminous mixtures.

Table 1. Geometrical characteristics of tested GB3 and GB5 specimens

Mixture	Name	Mass (g)	Diameter (mm)	Length (mm)	G_{mb} [a]	G_{mm} [b]	Air voids (%)
GB3	GB3-TPE1	1,572	73.8	140.9	2.610	2.670	2.3
	GB3-TPE2	1,564	73.7	140.1	2.614		2.1
	GB3-ETS	1,375	74.0	123.0	2.615		1.5
GB5	GB5-TPE1	1,581	73.8	140.5	2.630	2.654	0.8
	GB5-TPE2	1,585	73.7	140.7	2.641		0.5
	GB5-TPE3	—	—	—	—		0.5
	GB5-ETS	1,425	74.0	125.9	2.644		0.7

[a]Bulk specific gravity.
[b]Maximum specific gravity.

Test Equipment and Measurement Setup

The setups and the instrumentation for measuring the stress-strain values, which were different for the two laboratories (ETS and TPE), are presented in Fig. 4. These systems were also used by Perraton et al. (2016), who described them in more detail.

Tests were conducted in axial strain–control mode using a sinusoidal cyclic signal. The specimens were placed in a thermal chamber to assure temperature regulation.

In both laboratories, the axial strain was measured in the middle part of the specimen using three extensometers [Figs. 4(a and b)] located at 120°, with initial lengths of 75 and 50 mm at TPE and ETS, respectively. The radial strains were measured in dir2 and dir3 using four noncontact sensors (NCS) at TPE. For each directions, two noncontact sensors were placed on a sample diameter in

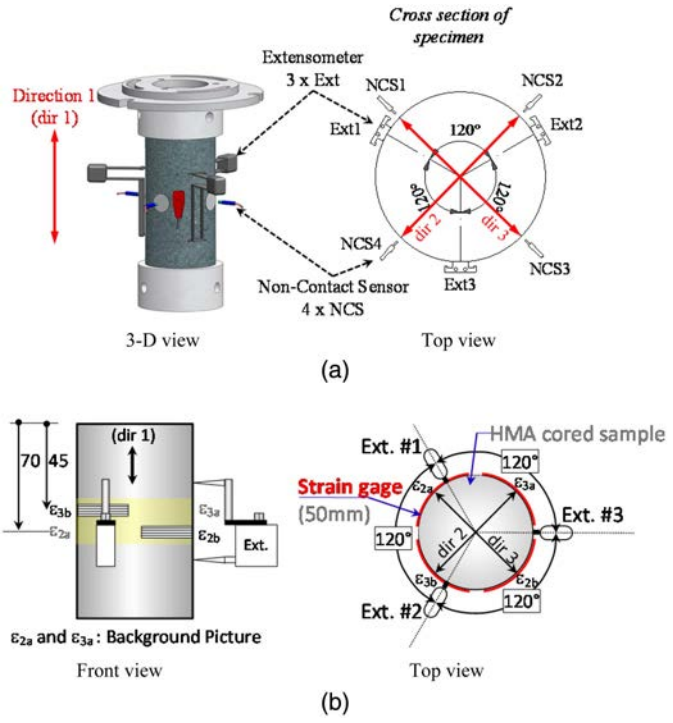

Fig. 4. Setup used by each laboratory: (a) TPE; and (b) ETS.

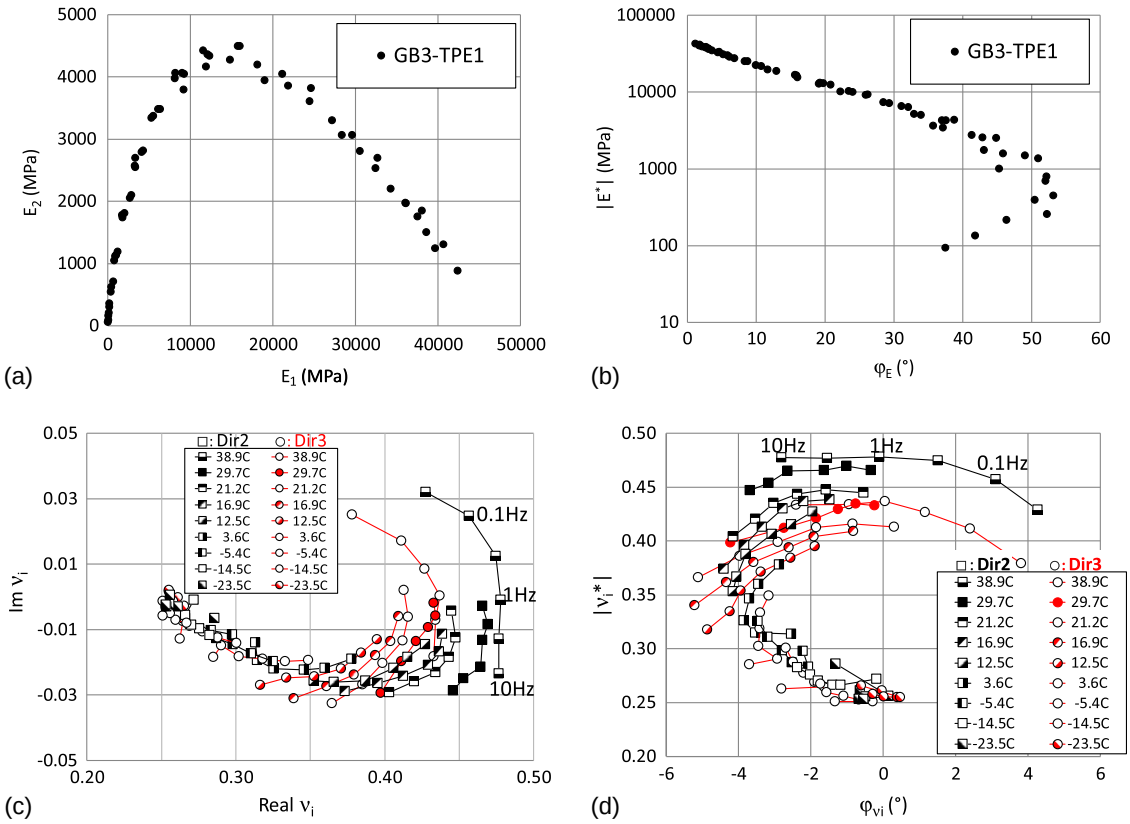

Fig. 5. Experimental values of complex Young's modulus and complex Poisson's ratios of sample GB3-TPE1: (a) Cole-Cole plane of E^*; (b) Black diagram of E^*; (c) Cole-Cole plane of ν_i^*; and (d) Black diagram of ν_i^*.

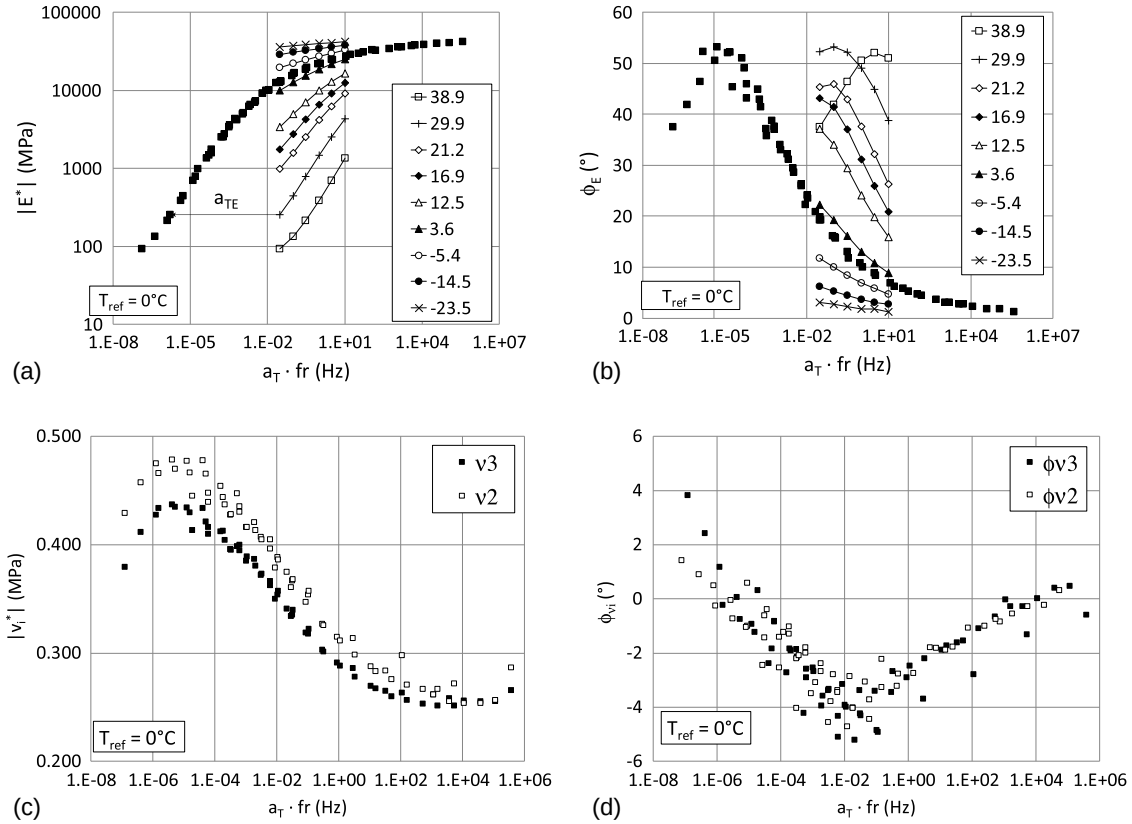

Fig. 6. Experimental results for sample GB3-TPE1: (a) $|E^*|$ isotherms and master curves; (b) ϕ_E isotherms and master curves; (c) master curves of $|\nu^*|$; and (d) master curves of $\phi_{\nu i}$.

opposite directions and aimed at two aluminum targets glued to the sample [Fig. 4(a), top view].

At ETS, the strains were measured in dir2 and dir3 using four strain gauges glued to the lateral surface of the samples. The length of the strain gauges was 50 mm. Two strain gauges were glued face-to-face on the cylinder wall and centered on the transverse axis for each transverse direction (dir2 and dir3) [Fig. 4(b)]. Two strain gauges (ε_{3a} and ε_{3b}) were placed face-to-face 45 mm from the top surface of the sample, and the two others were placed at 70 mm (ε_{2a} and ε_{2b}). The variations in the strain gauges due to temperature effects were considered in the analysis.

Tests were carried out at six frequencies (0.03, 0.1, 0.3, 1, 3, and 10 Hz), and at nine temperatures (−25°C to 40°C) and three temperatures (0°C, 15°C, and 30°C) at TPE and ETS, respectively. The sinusoidal axial strain (average of the three extensometers) was used to monitor the amplitude of axial strain during cyclic loading. To limit any bias that could exist for this type of test (e.g., heating due to viscous dissipation, thixotropy, and so on) (Di Benedetto et al. 2011; Nguyen et al. 2012; Mangiafico et al. 2015; Babadopulos et al. 2017), fewer than 100 cycles were applied at each testing frequency. The data acquisition and the analysis procedure were detailed by Perraton et al. (2016).

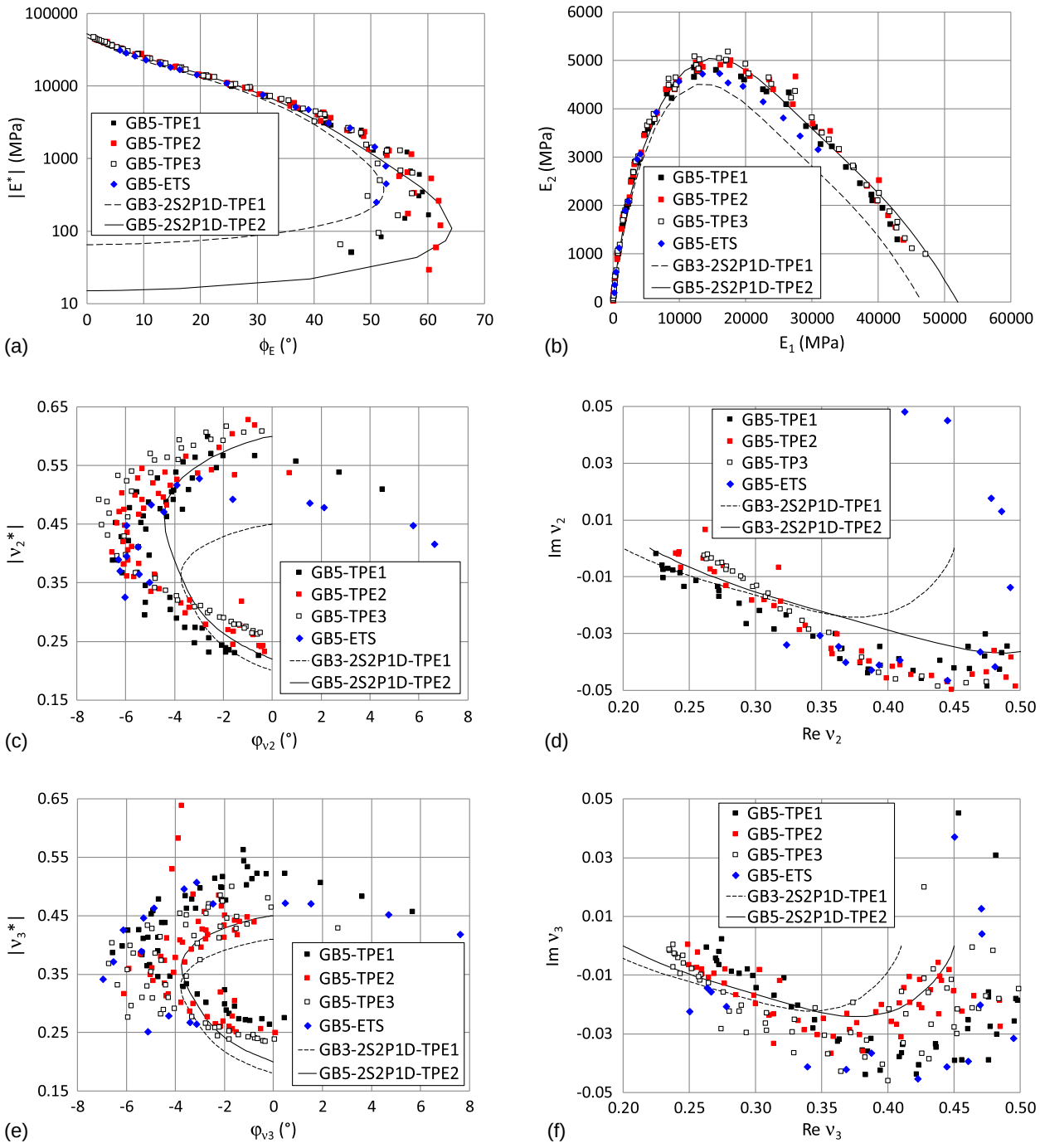

Fig. 7. Results of 2S2P1D model for GB5 samples (continuous lines) and GB3 samples (dashed lines): (a) complex modulus in Black diagram; (b) complex modulus in Cole-Cole plot; (c) complex Poisson's ratio in Black diagram for Direction 2 (ν_2); (d) complex Poisson's ratio in Cole-Cole plot for ν_2; (e) complex Poisson's ratio in Black diagram for Direction 3 (ν_3); and (f) complex Poisson's ratio in Cole-Cole plot for ν_3.

Experimental Results

In addition to analysis of the material behavior, which was the aim of this study, reproducibility of the tests between the two laboratories was checked. Repeatability was also checked at TPE, where one and two replicate tests for the GB3 and GB5 mixtures, respectively, were conducted.

Results for GB3-TPE1 Test

Figs. 5(a and b) show a unique curve in the Cole-Cole plane and in the Black diagram of the GB3-TPE1 test results. The same trend was found for all specimens of GB3 and GB5 mixtures tested at both laboratories. These unique curves indicate that the materials were thermorheologically simple and respected the time–temperature superposition principle (TTSP). Master curves were plotted at chosen reference temperature (T_{ref}) considering the shift factor a_T.

Figs. 5(c and d) show the Poisson's ratios obtained from the radial measurements (in dir2 and dir3) in Cole-Cole and Black diagrams. A unique curve can also be considered as a first approximation, which reveals that the Poisson's ratios in Directions 2 and 3 also respected the time–temperature superposition principle. The evolution of the complex Poisson's ratios was opposite that observed for the complex Young's modulus. The values of the norm increased with frequency and decreased with temperature.

The $|E^*|$ and ϕ_E master curves obtained for specimen GB3-TPE1 at the reference temperature (T_{ref}) 0°C are plotted in Figs. 6(a and b). The norm of complex modulus increased with frequency and decreased with temperature, which was expected; ϕ_E increased and then decreased when the equivalent frequency increased.

The $|\nu^*|$ and φ_ν master curves for Directions 2 and 3 of GB3-TPE1 sample are plotted at $T_{\text{ref}} = 0$°C in Figs. 6(c and d). As shown by Di Benedetto et al. (2007a), the same shift factor a_T was used for E^* and ν^*.

Perraton et al. (2016) provided a more extensive analysis for GB3 data. They found no significant differences between the complex Poisson's ratios evaluated in the two orthogonal directions. They also reported results obtained for complex Young's modulus and complex Poisson's ratios measured by five laboratories participating in a round-robin test within RILEM Technical Committee SIB activities.

Black and Cole-Cole Diagrams for GB5 Mixture

To check the repeatability and reproducibility of the complex Poisson's ratios of the GB5 mixture, three samples were tested by TPE and one sample was tested by ETS. Black and Cole-Cole diagrams are plotted in Fig. 7; the complex Young's modulus results for all tested samples were very close both in Cole-Cole plane [Fig. 7(b)] and Black diagram [Fig. 7(a)]. In Figs. 7(a and b), the dashed line indicates the simulation of GB3 results obtained with the 2S2P1D model, and the continuous line represents simulation of GB5 results with the 2S2P1D model.

Figs. 7(c–f) show the results for the complex Poisson's ratios in Directions 2 and 3. Some scattering is observed in these figures, which can be explained by the accuracy limit of the measurement system. The tests were performed at an axial strain amplitude of about 80 μm/m in order to remain within the linear domain. Because the magnitude of the radial strain is often less than half that in the axial direction, measured changes in diameter are quite small. This explains why great accuracy is needed for this measurement and why some scattering is hardly unavoidable (Graziani et al. 2017).

As shown previously, complex Poisson's ratios are a function of temperature and frequency and respect the time–temperature principle. Taken as a whole, the norms of the complex Poisson's ratio values were in the range 0.20–0.65, increasing with increasing temperature and decreasing with increasing frequency. In the Black and Cole-Cole diagrams, the complex Poisson's ratio data can be considered within the range of scattering for all GB5 samples. The Poisson's ratio values for Direction 2 were somewhat different from those for Direction 3. This difference may indicate anisotropy of the material. This point is treated in the last section of this paper.

The complex Young's modulus data from the two laboratories were very close (Fig. 7). Regarding the complex Poisson's ratios, all the data were within the scatter. These results indicate that the tests on the GB5 material had good reproducibility and good repeatability.

E^* and ν^* Shift Factor for GB3 and GB5 Materials

Fig. 8 shows that the experimental shift factor (a_{TE}) used to establish the master curves of $|E^*|$, $|\nu^*|$, ϕ_E, and ϕ_ν at $T_{\text{ref}} = 0$°C was the same for all tested samples of GB3 and GB5 mixtures. This confirms that a_{TE} is fixed by the bitumen and that the granular skeleton has negligible influence on this parameter. The shift factor was modeled with the classical WLF equation (Ferry 1980)

$$\log(a_T) = \frac{-C_1(T - T_{\text{ref}})}{C_2 + (T - T_{\text{ref}})} \tag{10}$$

Table 2 reports the C_1 and C_2 values for the GB3 and GB5 mixtures determined at 0°C (T_{ref}).

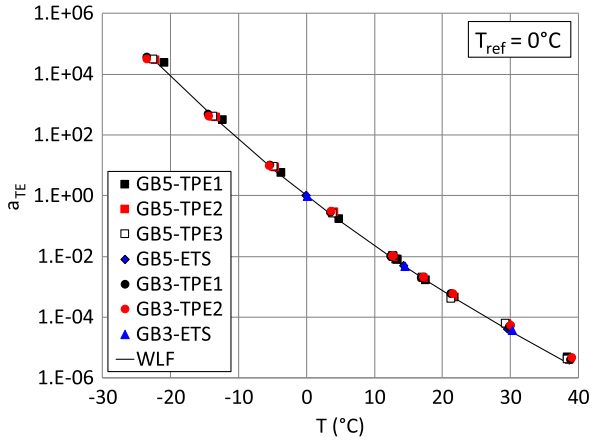

Fig. 8. Shift factors (a_{TE}) for all tested samples of GB3 and GB5 mixtures. The line represents the WLF fitting curve [Eq. (10)].

Table 2. WLF constants at reference temperature 0°C for GB3 and GB5 samples

WLF constant	Value
C_1	29.45
C_2	174.4
T_{ref} (°C)	0

Master Curves of Complex Young's Modulus and Complex Poisson's Ratios for GB5 Samples

In the small strain domain, the behavior of the binder is generally linear, and the TTSP can be considered (Nguyen et al. 2013). Only a single variable, namely the equivalent frequency (fr_{eq}), considers the effect of both temperature and frequency because the equivalent frequency is the product of the shift factor a_{TE}, which is a function of the temperature (T) and the chosen reference temperature (T_{ref}), by frequency (fr)

$$fr_{eq} = a_{TE} fr \tag{11}$$

Master curves obtained from the results of the tested samples of the GB5 mixture are reported in Fig. 9 at a reference temperature of 0°C. The master curves of the six parameters ($|E^*|$, $|\nu_2^*|$, $|\nu_3^*|$, ϕ_E, $\phi_{\nu 2}$, and $\phi_{\nu 3}$) are plotted in Figs. 9(a–f) as a function of the equivalent frequency [Eq. (11)]. The 2S2P1D model simulation of the GB5-TPE2 sample is indicated by continuous line, and the 2S2P1D model simulation of the GB3-TPE1 sample is plotted

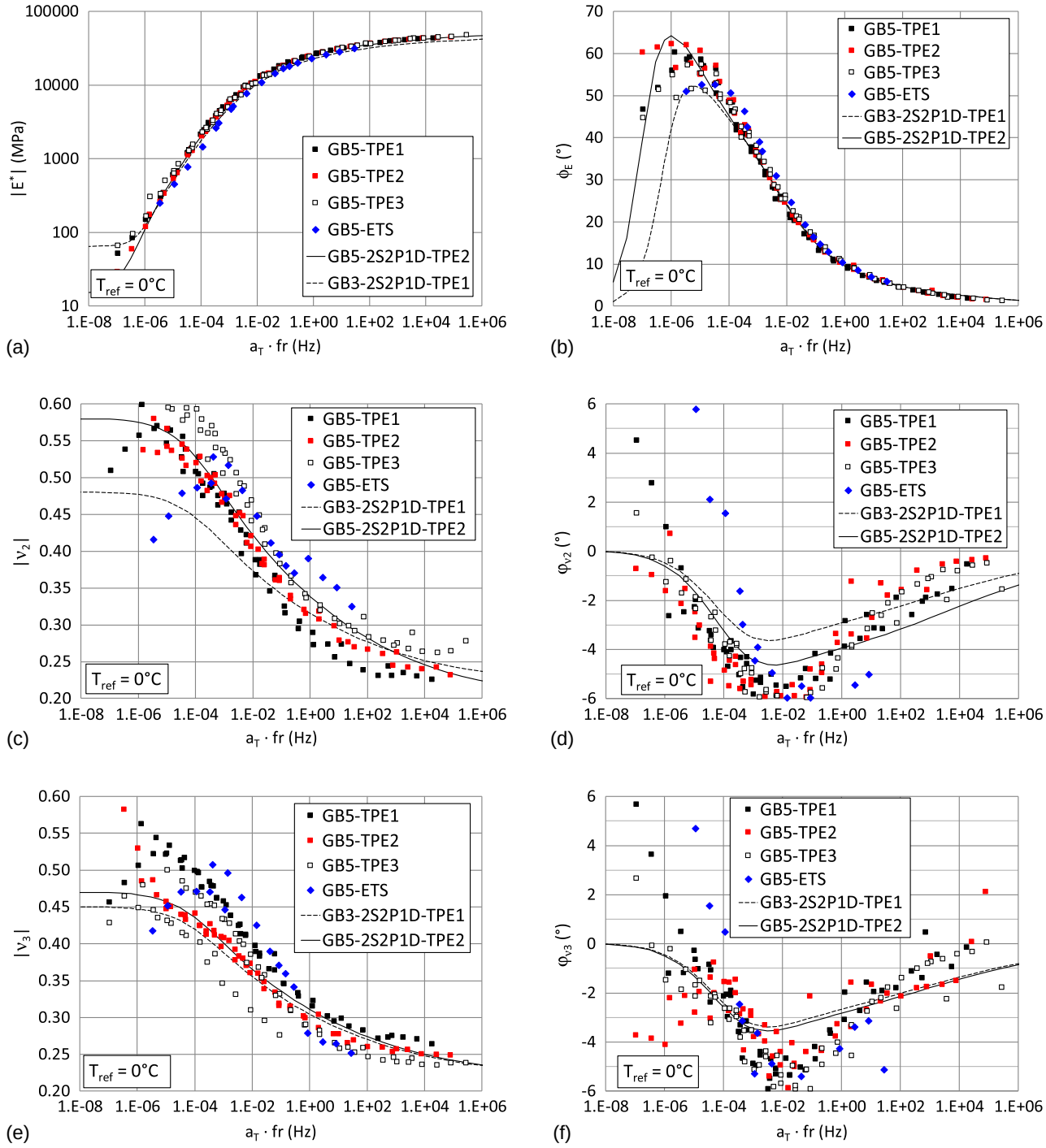

Fig. 9. Master curves for GB5 tested samples (data points) and 2S2P1D simulation curves for GB5-TPE2 (solid line) and GB3-TPE1 (dashed lines): (a) norm of complex modulus; (b) phase angles of complex modulus; (c) norm of complex Poisson's ratio ν_2^*; (d) phase angle of complex Poisson's ratios ν_2^*; (e) norm of complex Poisson's ratio ν_3^*; and (f) phase angles of complex Poisson's ratios ν_3^*.

Table 3. 2S2P1D model k, h, δ, and β constants for GB3 and GB5 tested samples

Constant	Value
k	0.15
h	0.52
δ	1.54
β	100

as a dashed line. The 2S2P1D model constants are listed in Tables 2–4. Scattering was also observed for the Poisson's ratio in Fig. 9. This is explained by the same factors described previously for the Cole-Cole and Black diagrams (Fig. 7).

Normalized Complex Young's Modulus of GB3 and GB5 Mixtures

Pouget et al. (2010) proposed normalizing the complex Young's modulus E^*_{norm} [Eq. (12)]. Pham et al. (2015a) showed that the curves obtained from normalized values in Cole-Cole and Black diagrams are fixed only by the bitumen and are independent of the granular skeleton. The same bitumen was used for the GB3 and GB5 samples, and Fig. 10 confirms that a unique curve was obtained in the Cole-Cole and Black representations for all tested materials. The only parameters needed to obtain normalized complex modulus [Eq. (12)] are E_{00} (the static modulus obtained at very low and/or high temperature) and E_0 (the glassy modulus obtained at very high and/or very low temperature). An implication of the existence of a unique curve in normalized axes is the consideration of a unique set of k, h, δ, and β constants for 2S2P1D modelling of all tested mixtures. These constants are reported in Table 3

$$E^*_{\text{Norm}} = \frac{E^* - E_{00}}{E_0 - E_{00}} \tag{12}$$

Fig. 10 confirms that the bitumen phase drives the viscoelastic behavior when expressed in normalized axes of the asphalt mixture, regardless of their granular skeleton. From Eqs. (7) and (8), the influence of the granular skeleton can be evaluated considering the evolution of the static modulus (E_{00}), the static Poisson's ratio (ν_{00}) in Directions 2 and 3, the glassy modulus (E_0), the glassy Poisson's ratio (ν_0) in Directions 2 and 3, and the 2S2P1D characteristic time values at a given reference temperature (τ_{0E} and $\tau_{0\nu}$). These constants are analyzed in next section.

Static (E_{00} and ν_{00}), Glassy (E_0 and ν_0), and Characteristic Time (τ_{0E} and $\tau_{0\nu}$) Values for GB3 and GB5 Samples

The obtained static (E_{00} and ν_{00}), glassy (E_0 and ν_0), and characteristic time (τ_{0E} and $\tau_{0\nu}$) values [Eqs. (7) and (8)] are presented in Table 4 for the tested GB3 and GB5 samples.

Static Young's Modulus

No clear evolution of static modulus E_{00} for both mixtures could be obtained from the data. Previous studies revealed that the degree of uncertainty is significantly high for E_{00} value determination

Table 4. Static (E_{00} and ν_{00}), glassy (E_0 and ν_0), and 2S2P1D characteristic time (τ_{0E} and $\tau_{0\nu}$) values determined at 0°C for GB3 and GB5 mixtures in Directions 2 and 3

					dir3:ν_3			dir2:ν_2		
Sample	Air voids (%)	E_{00} (MPa)	E_0 (MPa)	τ_{0E} (s)	ν_{00}	ν_0	$\tau_{0\nu}$ (s)	ν_{00}	ν_0	$\tau_{0\nu}$ (s)
GB5-TPE1	0.8	25	51,000	6.5	0.54	0.21	194	0.57	0.18	194
GB5-TPE2	0.5	15	52,000	5.0	0.47	0.22	150	0.58	0.20	150
GB5-TPE3	0.5	50	52,000	4.4	0.52	0.20	133	0.53	0.22	133
GB5-ETS	0.7	65	50,000	12.8	0.56	0.19	385	0.56	0.24	385
GB3-TPE1	2.3	65	46,600	4.6	0.45	0.22	137	0.48	0.22	137
GB3-TPE2	2.1	50	47,000	4.96	0.47	0.23	148	0.47	0.23	148
GB3-ETS	1.5	65	46,500	14.0	0.48	0.20	420	0.45	0.19	420

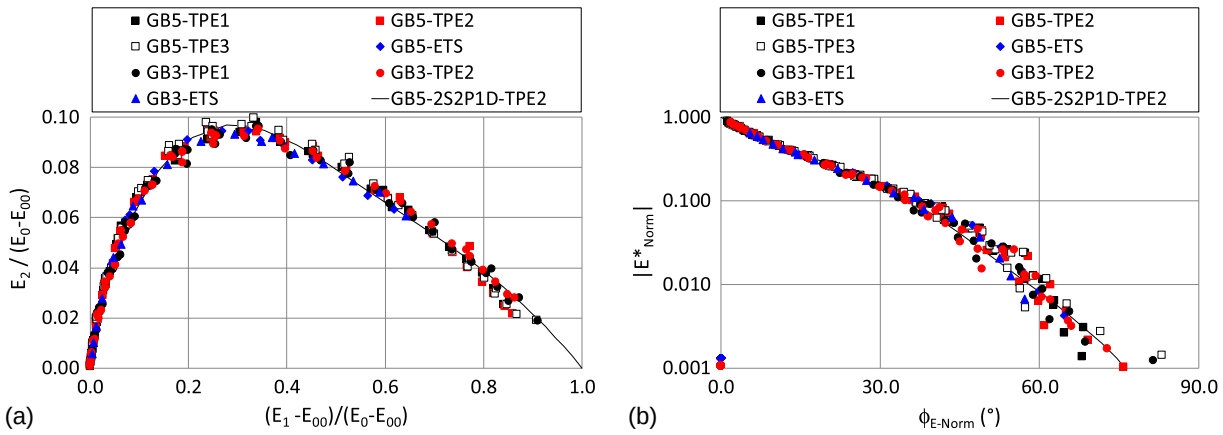

Fig. 10. Normalized complex Young's modulus data of GB3 and GB5 mixtures: (a) Cole-Cole plane; and (b) Black diagram. The line represents the 2S2P1D simulation [Eqs. (7) and (11)].

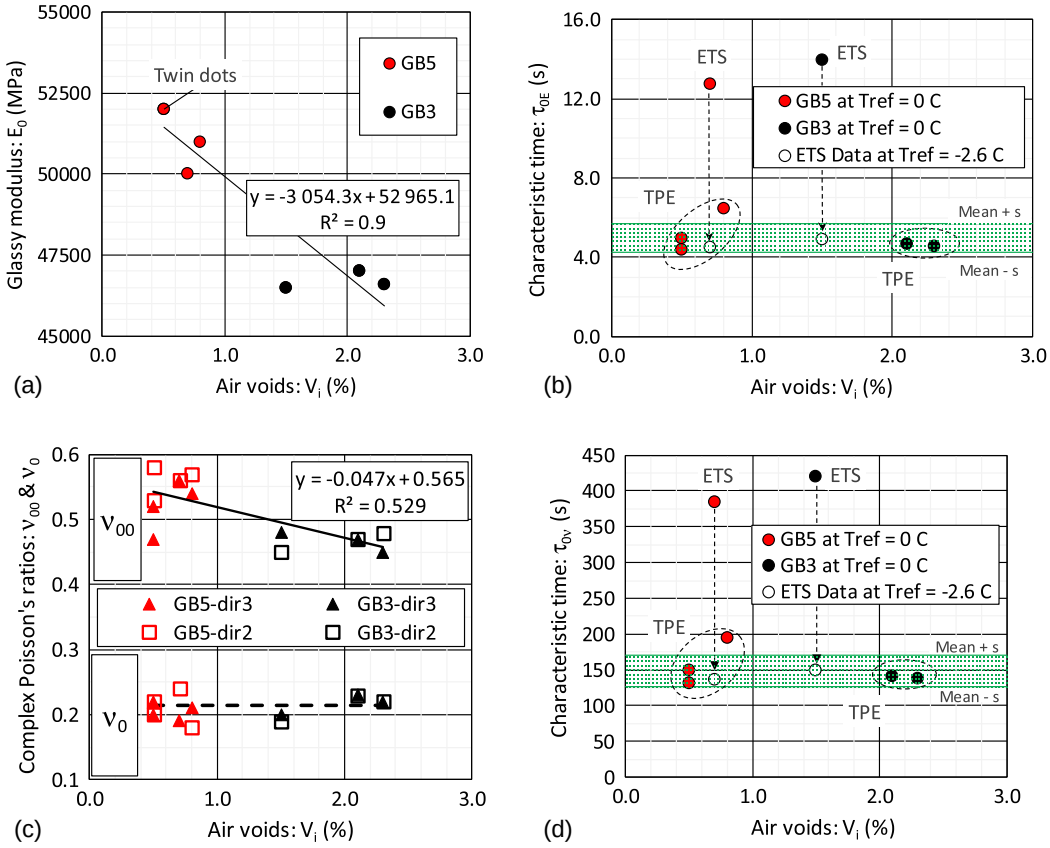

Fig. 11. Complex Young's modulus and complex Poisson's ratios constants of tested samples as a function of air-void content: (a) glassy Young's modulus (E_0); (b) Young's modulus characteristic time at T_{ref} (τ_{0E}); (c) glassy Poisson's ratios ν_0 and ν_{00} in Directions 2 and 3, respectively; and (d) Poisson's ratios characteristic time at T_{ref} ($\tau_{0\nu}$).

(high temperatures and/or low frequencies) due to creep and very soft properties of the mixtures at high temperature.

Glassy Young's Modulus

Fig. 11(a) plots E_0 values as a function of void content. Some authors reported a linear decrease of E_0 with an increase of void content. For example, Moutier (1991) found a slope of about 2,000 MPa per percentage void content decrease and Pham et al. (2015a) indicated a decrease of about 1,500 MPa per percentage void content decrease. Fig. 11(a) has a slope of 3,054 MPa per percentage void content decrease. This slope can be considered within the range of previously observed values. It is hypothesized that the difference in E_0 values observed between the GB3 and GB5 mixtures is independent of aggregates gradation and can be explained only by void content difference. It is worth checking this hypothesis.

Young's Modulus Characteristic Time Value

Fig. 11(b) shows the characteristic time values (τ_{0E}) of all tested samples determined at a reference temperature $T_{\text{ref}} = 0$°C. If the results from each laboratory (TPE and ETS) are considered separately, no significant difference was found between the GB3 and GB5 mixtures. However, there was a clear difference between values from each of the two laboratories. The ETS results from the two laboratories at a reference temperature of −2.6°C [Fig. 11(b), hollow circles] were very similar. This output, previously discussed by Perraton et al. (2016) for GB3 mixture, may be explained by temperature regulation that differed by about 2.6°C between the two laboratories. Taking into account the ETS-corrected values, the mean characteristic time value for the two tested mixtures (GB3 and GB5) was 4.97 s, with a standard deviation of 0.71 s. Fig. 11(b) indicates an interval of one standard deviation on each side of the average. The calculated temperature interval associated with this interval was ±0.40°C. Based on this result, a unique characteristic time value of 5.0 can be considered for the two tested mixtures (GB3 and GB5).

Poisson's Ratio Constants in dir2 and dir3

The relationship between the air voids content and the ν_{00} and ν_0 values is plotted in Fig. 11(c). Similar results were obtained in the two laboratories. Static (ν_{00}) values were higher than glassy (ν_0) values, but no significant difference was observed between Directions 3 and 2. The glassy Poisson's ratios (ν_0) were very close for all samples, whereas the static Poisson's ratios decreased when void content increased.

Poisson's Ratio Characteristic Time Value

Fig. 11(d) shows the Poisson's ratio characteristic time values ($\tau_{0\nu}$) of the GB3 and GB5 mixtures at the reference temperature ($T_{\text{ref}} = 0$°C). The ETS results from both laboratories at a reference temperature of −2.6°C were in the same range. The remark made for the Young's modulus characteristic time value (τ_{0E}) also applies for the Poisson's ratio characteristic time values ($\tau_{0\nu}$), confirming that a 2.6°C difference may exist between the thermal chambers of the two laboratories.

Table 5 gives average values that can be considered for 2S2P1D model simulation of each of the studied mixtures (GB3 and GB5).

Table 5. Average static, glassy, and characteristic time values selected for 2S2P1D model simulation of each mixture

				dir2:ν_2			dir3:ν_3			
Mixture	E_{00} (MPa)	E_0 (MPa)	τ_{0E} (s)	ν_{00}	ν_0	$\tau_{0\nu}$ (s)	ν_{00}	ν_0	$\tau_{0\nu}$ (s)	T_{ref} (°C)
GB3	60	46,700	5.0	0.47	0.21	150	0.47	0.22	150	0
GB5	39	51,250	5.0	0.56	0.21	150	0.52	0.21	150	0

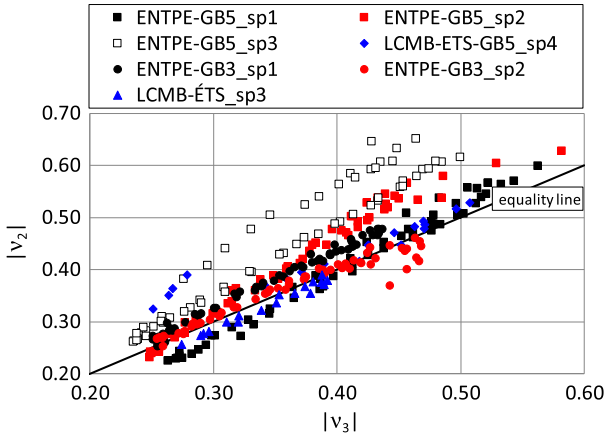

Fig. 12. Norms of complex Poisson's ratio in dir2 and dir3.

Results on Anisotropic Properties of GB3 and GB5 Samples

Fig. 12 shows the relationship between the norm of the complex Poisson's ratio in dir2 ($|\nu_2|$) and the norm of the complex Poisson's ratio in dir3 ($|\nu_3|$). Most of the data were close to the equality line, which indicates that the anisotropy effect on the Poisson's ratio, if any, was negligible.

Conclusions

This paper analyzed the results of the complex Young's modulus and complex Poisson's ratios of two different types of hot mixture asphalt (HMA) made with the same bitumen but produced with different aggregate gradations. The two tested bituminous mixtures (GB3 and GB5) are used in France as base-course material in asphalt-structure pavements. Sinusoidal axial strain loading was applied to cylindrical samples. In addition to axial stress and strain values, the transverse strains of the cored samples were measured in two orthogonal directions (dir2 and dir3).

From the obtained results, it can be concluded that

- The GB3 and GB5 mixtures behave very much like a thermo-rheological simple material: the time–temperature superposition principle (TTSP) is applicable.
- The same shift factor (a_{TE}) was obtained for the two mixtures both for Young's modulus and Poisson's ratio in Directions 2 and 3, which confirms that this parameter is fixed by the binder only.
- The norm of the Poisson's ratio values varied in the range from 0.20 to 0.55, increasing with temperature and decreasing with frequency;
- Based on the normalized complex modulus curves that were superimposed for all GB3 and GB5 tested samples, a unique set of k, h, δ, and β constants can be considered for the 2S2P1D linear viscoelastic model. This result confirms that the bitumen phase drives the viscoelastic behaviour of the asphalt mixture, regardless of the granular skeleton.
- Glassy Young's modulus evolution is explained only with void content;
- Complex Poisson's ratios from dir2 and dir3 were very similar for the GB3 and GB5 samples.
- The reproducibility between the two laboratories was good if a difference of about 2.6°C, which probably exists between the two thermal chambers, is considered.

References

Airey, G., B. Rahimzadeh, and A. Collop. 2003. "Viscoelastic linearity limits for bituminous materials." In *6th Int. RILEM Symp. on Performance Testing and Evaluation of Bituminous Materials*, 331–338. Bagneux, France: RILEM Publications SARL.

Aurangzeb, Q., H. Ozer, I. L. Al-Qadi, and H. H. Hilton. 2017. "Viscoelastic and Poisson's ratio characterization of asphalt materials: Critical review and numerical simulations." *Mater. Struct.* 50 (1): 49. https://doi.org/10.1617/s11527-016-0881-x.

Babadopulos, L., C. Sauzéat, and H. Di Benedetto. 2017. "Softening and local self-heating of bituminous mixtures during cyclic loading." Supplement, *Road Mater. Pavement Des.* 18 (S2): 164–177. https://doi.org/10.1080/14680629.2017.1304260.

CEN (European Committee for Standardization). 2007a. *Mélange bitumineux—Méthodes d'essai pour mélange hydrocarboné à chaud - Partie 33: confection d'éprouvettes au compacteur de plaque*. NF EN 12697-33+A1. Brussels, Belgium: CEN.

CEN (European Committee for Standardization). 2007b. *Mélanges bitumineux—Méthodes d'essai pour mélange hydrocarboné à chaud - Partie 35: malaxage en laboratoire*. NF EN 12697-35+A1. Brussels, Belgium: CEN.

Di Benedetto, H., B. Delaporte, and C. Sauzeat. 2007a. "Three-dimensional linear behaviour of bituminous materials: Experiments and modelling." *Int. J. Geomech.* 7 (2): 149–157. https://doi.org/10.1061/(ASCE)1532-3641(2007)7:2(149).

Di Benedetto, H., N. Mondher, C. Sauzéat, and F. Olard. 2007b. "Three-dimensional thermo-viscoplastic behaviour of bituminous materials—The DBN model." *Road Mater. Pavement Des.* 8 (2): 285–315. https://doi.org/10.1080/14680629.2007.9690076.

Di Benedetto, H., Q. T. Nguyen, and C. Sauzeat. 2011. "Nonlinearity, heating, fatigue and thioxotropy during cyclic loading of asphalt mixtures." *Road Mater. Pavement Des.* 12 (1): 129–158. https://doi.org/10.1080/14680629.2011.9690356.

Di Benedetto, H., F. Olard, C. Sauzéat, and B. Delaporte. 2004. "Linear viscoelastic behaviour of bituminous materials: From binders to mixes." Supplement, *Road Mater. Pavement Des.* 5 (S1): 163–202. https://doi.org/10.1080/14680629.2004.9689992.

Di Benedetto, H., M. N. Partl, L. Francken, and C. De La Roche Saint André 2001. "Stiffness testing for bituminous mixtures." *Mater. Struct.* 34 (2): 66–70. https://doi.org/10.1007/BF02481553.

Di Benedetto, H., C. Sauzéat, and P. Clec'h. 2016. "Anisotropy of bituminous mixture in the linear viscoelastic domain." *Mech. Time-Depend. Mater.* 20 (3): 281–297. https://doi.org/10.1007/s11043-016-9305-0.

Ferry, J. D. 1980. *Viscoelastic properties of polymers*. 3rd ed. New York: Wiley.

Gayte, P., H. Di Benedetto, C. Sauzéat, and Q. T. Nguyen. 2016. "Influence of transient effects for analysis of complex modulus tests on bituminous mixtures." *Road Mater. Pavement Des.* 17 (2): 271–289. https://doi.org/10.1080/14680629.2015.1067246.

Godenzoni, C., A. Graziani, and D. Perraton. 2017. "Complex modulus characterisation of cold-recycled mixtures with foamed bitumen and different contents of reclaimed asphalt." *Road Mater. Pavement Des.* 18 (1): 130–150. https://doi.org/10.1080/14680629.2016.1142467.

Graziani, A., et al. 2018. "Three-dimensional characterisation of linear viscoelastic properties of bituminous mixtures." Chap. 3 in Vol. 24 of *Testing and characterization of sustainable innovative bituminous materials and systems*, 75–125. Cham: Springer.

Graziani, A., M. Bocci, and F. Canestrari. 2014. "Complex Poisson's ratio of bituminous mixtures: Measurement and modelling." *Mater. Struct.* 47 (7): 1131–1148. https://doi.org/10.1617/s11527-013-0117-2.

Graziani, A., H. Di Benedetto, D. Perraton, C. Sauzéat, B. Hofko, L. D. Poulikakos, and S. Pouget. 2017. "Recommendation of RILEM TC 237-SIB on complex Poisson's ratio characterization of bituminous mixtures." *Mater. Struct.* 50 (2): 142. https://doi.org/10.1617/s11527-017-1008-8.

Gudmarsson, A., N. Ryden, H. Di Benedetto, and C. Sauzeat. 2015. "Complex modulus and complex Poisson's ratio from cyclic and dynamic modal testing of asphalt concrete." *Constr. Build. Mater.* 88: 20–31. https://doi.org/10.1016/j.conbuildmat.2015.04.007.

Gudmarsson, A., N. Ryden, H. Di Benedetto, C. Sauzeat, N. Tapsoba, and B. Birgisson. 2014. "Comparing linear viscoelastic properties of asphalt concrete measured by laboratory seismic and tension-compression tests." *J. Nondestr. Eval.* 33 (4): 571–582. https://doi.org/10.1007/s10921-014-0253-9.

Jiménez del Barco Carrión, A., D. Lo Presti, S. Pouget, G. Airey, and E. Chailleux. 2017. "Linear viscoelastic properties of high reclaimed asphalt content mixes with biobinders." *Road Mater. Pavement Des.* 18 (sup2): 241–251. https://doi.org/10.1080/14680629.2017.1304253.

Lachance-Tremblay, É., M. Vaillancourt, and D. Perraton. 2016. "Linear viscoelastic properties, low temperature and fatigue performances of asphalt mixture with recycled glass." In *Proc., ISAP 2016 Symp. Int. Society for Asphalt Pavements (ISAP)*, Lino Lakes, MN.

Lamothe, S., D. Perraton, and H. Di Benedetto. 2016. "Deterioration of HMA partially saturated with water or brine subjected to freeze-thaw cycles." In *Proc., 8th RILEM Int. Symp. on Testing and Characterization of Sustainable and Innovative Bituminous Materials*, edited by F. Canestrari and M. N. Partl, 705–717. Dordrecht, Netherlands: Springer.

Lamothe, S., D. Perraton, and H. Di Benedetto. 2017. "Degradation of hot mix asphalt samples subjected to freeze-thaw cycles and partially saturated with water or brine." *Road Mater. Pavement Des.* 18 (4): 849–864. https://doi.org/10.1080/14680629.2017.1286442.

Mangiafico, S., H. Di Benedetto, C. Sauzéat, F. Olard, S. Pouget, and L. Planque. 2014. "New method to obtain viscoelastic properties of bitumen blends from pure and reclaimed asphalt pavement binder constituents." *Road Mater. Pavement Des.* 15 (2): 312–329. https://doi.org/10.1080/14680629.2013.870639.

Mangiafico, S., C. Sauzeat, H. Di Benedetto, S. Pouget, F. Olard, and L. Planque. 2015. "Quantification of biasing effects during fatigue tests on asphalt mixes: Non-linearity, self-heating and thixotropy." Supplement, *Road Mater. Pavement Des.* 16 (S2): 73–99. https://doi.org/10.1080/14680629.2015.1077000.

Md. Yusoff, N. I., D. Mounier, G. Marc-Stéphane, M. Rosli Hainin, G. D. Airey, and H. Di Benedetto. 2013. "Modelling the rheological properties of bituminous binders using the 2S2P1D Model." *Constr. Build. Mater.* 38: 395–406.

Moutier, F. 1991. "Étude statistique de l'effet de composition sur comportement fatigue et module." [In French.] *Bulletin de Liaison des Laboratoire des Ponts et Chaussées* 172: 33–41.

Nguyen, Q. T., H. Di Benedetto, and C. Sauzéat. 2012. "Determination of thermal properties of asphalt mixtures as another output from cyclic tension-compression test." *Road Mater. Pavement Des.* 13 (1): 85–103. https://doi.org/10.1080/14680629.2011.644082.

Nguyen, Q. T., H. Di Benedetto, and C. Sauzéat. 2015a. "Effect of fatigue cyclic loading on linear viscoelastic properties of bituminous mixtures." *J. Mater. Civ. Eng.* 27 (8): C4014003. https://doi.org/10.1061/(ASCE)MT.1943-5533.0000996.

Nguyen, Q. T., H. Di Benedetto, and C. Sauzéat. 2015b. "Linear and non-linear viscoelastic behavior of bituminous mixtures." *Mater. Struct.* 48 (7): 2339–2351. https://doi.org/10.1617/s11527-014-0316-5.

Nguyen, Q. T., H. Di Benedetto, C. Sauzéat, M. L. Nguyen, and T. T. N. Hoang. 2017. "3D complex modulus tests on bituminous mixture with sinusoidal loadings in tension and/or compression." *Mater. Struct.* 50 (1): 98. https://doi.org/10.1617/s11527-016-0970-x.

Nguyen, Q. T., H. Di Benedetto, C. Sauzéat, and N. Tapsoba. 2013. "Time temperature superposition principle validation for bituminous mixes in the linear and nonlinear domains." *J. Mater. Civ. Eng.* 25 (9): 1181–1188. https://doi.org/10.1061/(ASCE)MT.1943-5533.0000658.

Olard, F., and H. Di Benedetto. 2003. "General '2S2P1D' model and relation between the linear viscoelastic behaviors of bituminous binders and mixes." *Road Mater. Pavement Des.* 4 (2): 185–224. https://doi.org/10.1080/14680629.2003.9689946.

Olard, F., F. Huon, D. Perraton, and C. Billet. 2010. "On the optimization of the aggregate packing for the design of self-blocking high-performance asphalt." In *Proc., 11th Conf. of the Int. Society of Asphalt Pavement (ISAP)*. Lino Lakes, MN.

Olard, F., and D. Perraton. 2010. "On the optimization of the aggregate packing characteristics for the design of high-performance asphalt concretes." Supplement, *Road Mater. Pavement Des.* 11 (S1): 145–169. https://doi.org/10.1080/14680629.2010.9690330.

Perraton, D., et al. 2016. "3Dim experimental investigation of linear viscoelastic properties of bituminous mixtures." *Mater. Struct.* 49 (11): 4813–4829. https://doi.org/10.1617/s11527-016-0827-3.

Perraton, D., M. Meunier, and A. Carter. 2007. "Application des méthodes d'empilement granulaire à la formulation des SMA, Bull. des Labo. des Ponts et Chaussées." 270–271: 87–108.

Pham, N. H., C. Sauzéat, H. Di Benedetto, J. A. Gonzalez-Leon, G. Barreto, A. Nocolai, and M. Jajubowski. 2015a. "RAP and additive influence on 3D linear behaviour of warm bituminous mixtures." *Road Mater. Pavement* 16 (3): 569–591. https://doi.org/10.1080/14680629.2015.1021108.

Pham, N. H., C. Sauzéat, H. Di Benedetto, J. A. González-León, G. Barreto, A. Nicolaï, and M. Jakubowski. 2015b. "Analysis and modeling of 3D complex modulus tests on hot and warm bituminous mixtures." *Mech. Time-Depend. Mater.* 19 (2): 167–186. https://doi.org/10.1007/s11043-015-9258-8.

Pouget, S., C. Sauzeat, H. Di Benedetto, and F. Olard. 2010. "From the behavior of constituent materials to the calculation and design of orthotropic bridge structures." Supplement, *Road Mater. Pavement Des.* 11 (S1): 111–144. https://doi.org/10.1080/14680629.2010.9690329.

Pouget, S., C. Sauzeat, H. Di Benedetto, and F. Olard. 2012. "Modeling of viscous bituminous wearing course materials on orthotropic steel deck." *Mater. Struct.* 45 (7): 1115–1125. https://doi.org/10.1617/s11527-011-9820-z.

Riahi, E., F. Allou, R. Botella, F. Fakhari Tehrani, F. Dubois, J. Absi, C. Petit, and F. E. Pérez-Jiménez. 2017. "Modelling self-heating and thixotropy phenomena under the cyclic loading of asphalt." Supplement, *Road Mater. Pavement Des.* 18 (S2): 155–163. https://doi.org/10.1080/14680629.2017.1305145.

Riccardi, C., A. Cannone Falchetto, M. Losa, and M. Wistuba. 2018. "Development of simple relationship between asphalt binder and mastic based on rheological tests." *Road Mater. Pavement Des.* 19 (1): 18–35. https://doi.org/10.1080/14680629.2016.1230514.